AIAA JOURNAL
Vol. 32, No. 6, June 1994

Fluctuating Wall Pressures near Separation in Highly Swept Turbulent Interactions

J. D. Schmisseur*
Wright-Patterson Air Force Base, Dayton, Ohio 45433
and
D. S. Dolling†
University of Texas at Austin, Austin, Texas 78712

Fluctuating wall pressures have been measured in Mach 5 interactions generated by sharp, unswept fins at angles of attack of 16 to 28 deg. The results show that rms pressure distributions, like the mean, can be collapsed in conical coordinates. The wall pressure signal near separation is intermittent and is qualitatively similar to that measured in unswept interactions and other swept flows. However, the dominant separation shock frequencies in the swept flows are up to an order of magnitude higher than those in unswept interactions under identical incoming flow conditions. In light of the present observations, it appears that an earlier remark, by Gilson and Dolling, that separation is characterized by a "shuddering compression system, in contrast to a translating separation shock" is erroneous due to a combination of weak shock strength and inadequate spatial resolution. Furthermore, although the maximum rms pressure near separation increases with increasing interaction strength, as in swept compression ramp flows, comparison of data from the two flow types indicates that the appropriate correlating parameter is the interaction sweepback angle.

Introduction

WITH the increasing prominence of high-speed vehicles in the national agenda, interest in shock-wave/turbulent boundary-layer interactions remains strong. Such interactions can generate large amplitude fluctuating pressure loads (up to 185 dB) and high heating rates whose magnitudes are critical to the prediction of aeroacoustic loads and structural fatigue. To optimize aerodynamic/structural design an improved understanding of the dynamics of the shock-wave/turbulent boundary-layer interaction is essential. One of the most commonly studied swept interactions is that caused by a sharp fin at angle of attack α mounted perpendicular to a flat test surface. This interaction, simply called the sharp fin or glancing shock interaction, is representative of the more complex interactions found in engine inlets and at fin/body junctions. Although much has been learned about the mean surface properties and flow structure,[1] questions remain regarding the unsteadiness of the interaction.

The dominant inviscid feature of the interaction is the planar shock wave attached to the fin leading edge. A standard measure of the interaction strength is given by M_n, the Mach number normal to the inviscid shock. The evolution of the interaction cross-plane flow structure as a function of M_n has been investigated by Alvi and Settles[2,3] using conical shadowgraphy and conical planar laser scattering. Results show that significant viscous effects are confined to the region near the fin leading edge and that after a certain radial distance the interaction becomes quasiconical. This region near the leading edge, called the inception region, has length *Li* and is a result of the dimension introduced into the flowfield by the incoming boundary layer thickness δ. Because of the inception region, the origin of the surface and flowfield features in the quasiconical far field is not coincident with the fin leading edge. Instead, they emanate from a virtual conical origin (VCO) just upstream of the fin leading edge along the extended inviscid shock trace (Figs. 1 and 2). As a result of the quasiconical symmetry of the interaction far field, a spherical/polar coordinate system with the origin located at the VCO (Fig. 1) is most appropriate for studying the interaction. Features of interest are then given in terms of angles relative to the freestream direction or test surface.

Pertinent features of the interaction footprint and the corresponding nomenclature are shown in Fig. 2. The upstream influence line, at angle β_{ui}, is the line along which the incoming surface streaklines initially deviate from the freestream direction, and correlates well with the line along which the mean surface pressure first increases. The primary separation line, at angle β_{s1}, appears as a coalescence of streaklines. Beneath the separated boundary layer, the flow forms a spiraling, helical vortex. Further details of the flow structure, deduced from both experiment and computation, can be found in Refs. 1–4.

To the authors' knowledge, studies of the unsteadiness of sharp fin interactions have been made in only three facilities. The first was made at Mach 3 at Princeton University, the results of which have been reported in Refs. 5–7. It was noted that the wall pressure signal near separation was intermittent, indicative of a translating separation shock wave. Since measurements were made at two

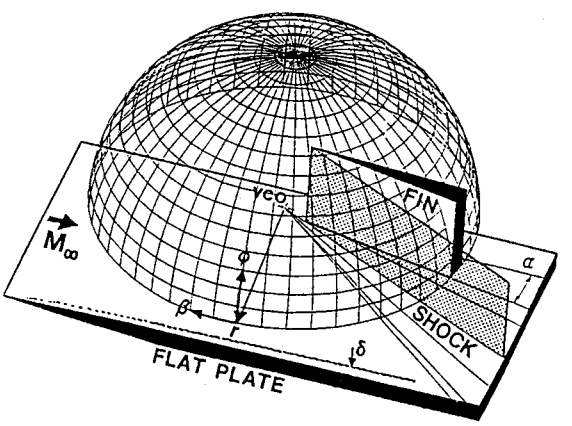

Fig. 1 Spherical/polar coordinate system.

Received Aug. 5, 1993; revision received Sept. 17, 1993; accepted for publication Jan. 20, 1994.

*Aerospace Engineer, Aeromechanics Division, Wright Laboratory/Flight Dynamics Directorate Aeromechanics Division, Experimental Facilities Research Branch. Member AIAA.

†Professor, Department of Aerospace Engineering and Engineering Mechanics, Center for Aeromechanics Research.

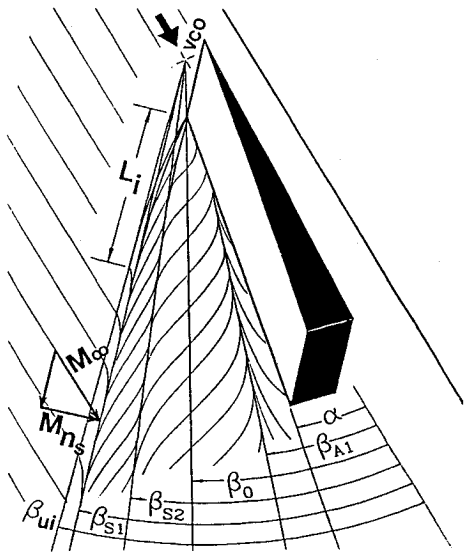

Fig. 2 Surface flow features.[1]

spanwise locations for only one fin angle of attack, questions concerning the radial evolution of the fluctuating wall pressure field could not be addressed. In later work at the University of Texas at Austin, exploratory experiments at Mach 5 yielded wall pressure signals near separation indicative of a quasisteady "shuddering" compression system rather than a translating separation shock wave.[8,9] Measurements were made along rays from the VCO, but the limited radial extent of the data and scatter prevented the authors from drawing a definitive conclusion regarding quasiconical symmetry of the fluctuating wall pressure field. The most recent study, which was published following completion of the current work, is that of Garg and Settles,[10] who present results for fin angles of attack of 10, 16, and 20 deg at Mach 3 and for 16 and 20 deg at Mach 4. In anticipation of quasiconical symmetry, transducers were installed along a circular arc centered at the fin leading edge. Measurements were made at only one radial location, and thus no proof of conical symmetry was provided. Also, the measured wall pressure signals near separation were not intermittent. The main focus of their effort was to explain the features of the mean and rms distributions using detailed flowfield maps developed in earlier work.[2,3]

The present study was an attempt to learn more about the unsteadiness of sharp fin-induced interactions and, we hope, clarify some issues arising from the earlier work of Tran et al.,[6] and Gibson and Dolling.[8,9] The following questions were addressed.

1) Does the rms of the wall pressure fluctuations, and hence the fluctuating load distribution, exhibit quasiconical symmetry similar to the mean wall pressure?

2) Is the initial compression region near separation characterized by a translating separation shock generating an intermittent pressure signal or by a quasisteady, shuddering compression wave system? Can both phenomena exist and is there a range of interaction sweep angles or shock strengths over which there is a transition from intermittent to quasisteady behavior?

3) In swept interactions, does the maximum rms in the vicinity of separation correlate with the overall inviscid pressure rise or is it dependent only on local conditions?

Experimental Program

A brief description of the experimental program is given next. Further details are given in Refs. 11 and 12.

Test Facilities and Flow Conditions

The experiments were conducted under approximately adiabatic wall temperature conditions in the Mach 5 blowdown tunnel of the University of Texas at Austin. The tunnel has a constant area test section that is 17.78 cm (7 in.) high by 15.24 cm (6 in.) wide and is located about 90 cm (36 in.) downstream of the nozzle throat. The nominal stagnation chamber pressure and temperature for the current work were 2.27 MPa (330 psia) and 635°R (353 K), respectively. The test section Mach number is 4.95. These conditions generate a freestream Reynolds number of approximately 48×10^6 m^{-1} (14.6×10^6 ft^{-1}).

The incoming tunnel floor boundary layer was turbulent and developed naturally without the need for trips. Pitot pressure and total temperature surveys in the undisturbed boundary layer show that the mean velocity profile closely matches the law of the wall/law of the wake. The properties of the boundary layer 9.5 cm (3.74 in.) downstream of the junction of the nozzle and test section are listed in Table 1. This position is 3.3 cm (1.3 in.) downstream of the fin leading edge.

Model

The shock generator was a stainless steel fin with an unswept, sharp leading edge mounted normal to the floor of the wind tunnel as shown in Fig. 3. The fin was 12.7 cm (5 in.) long, 7.62 cm (3 in.) high, and 1.25 cm (0.5 in.) thick, which was sufficiently small to start the tunnel at any required angle of attack yet large enough that the fin was effectively semi-infinite. The angle of attack mechanism was calibrated with a machinist's protractor, and it is estimated that the α is accurate to within $\pm$ 0.5 deg. At the maximum angle of attack, α = 28 deg, both the fin leading and trailing edges were more than 3.6 cm (1.4 in.) from the tunnel sidewalls, which was sufficient to avoid interference from the sidewall boundary layers.

Instrumentation and Data Acquisition

Fluctuating wall pressure measurements were made using Kulite Semiconductor Products, Inc., model XCQ-062-15A (0–15 psia, $0–1.03 \times 10^5$ Pa) and model XCQ-062-50A (0-50 psia,

Table 1 Undisturbed boundary-layer parameters

δ_0	1.51 cm	(0.59 in.)
δ^*	0.67 cm	(0.26 in.)
θ	6.6×10^{-2} cm	(2.6×10^{-2} in.)
Π	0.78	
H	10.2	
Re_θ	3.17×10^{-4}	
C_f	7.74×10^{-4}	

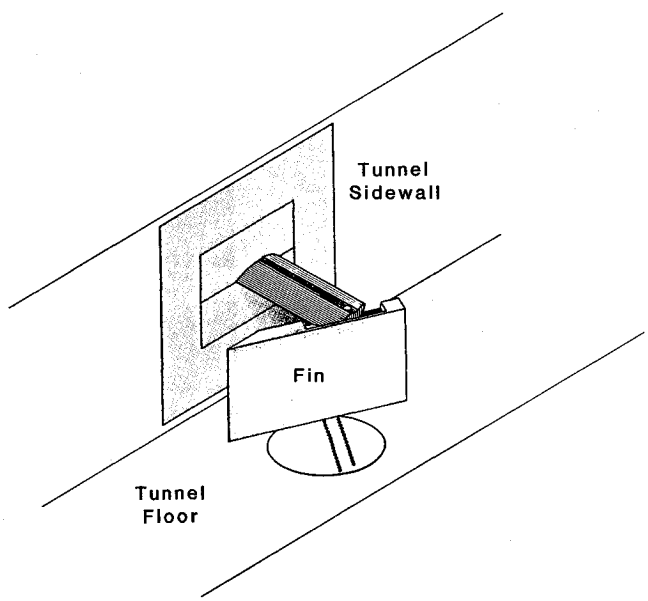

Fig. 3 Model arrangement.

0–3.44 $\times 10^5$ Pa) transducers. The transducers have a pressure-sensitive area 0.71 mm (0.028 in.) in diameter and an outer case diameter of approximately 1.63 mm (0.064 in.). Perforated screens above the diaphragm protect it from damage due to any dust particles in the flow but limit the frequency response of both transducer models to about 50 kHz. The transducers were calibrated statically on a daily basis using a Heise model 710A digital pressure gauge accurate to within 0.001 psia (7 Pa).

Transducer voltage output was amplified and low pass filtered before being digitized. Two LeCroy analog-to-digital (A/D) converters (model 6810 waveform recorders) with 12-bit resolution were used. Each A/D converter output 0–4095 "counts" for an input of 0–4 V. Data were taken at sampling rates of either 50 or 200 kHz per channel, and for each run 256 records of 1024 points were acquired. Typical noise on the data acquisition system varied between ±5 to 15 counts peak to peak, with a typical signal-to-noise ratio of about 100.

Data were acquired using six to eight transducers per run. The transducers were flush mounted along two straight rows in a rotatable plug (Fig. 4). The rows, labeled A and B in Fig. 4, were 0.508 cm and 1.524 cm from the center of the plug and had 23 and 20 transducer ports, respectively. All ports were spaced 0.292 cm (0.115 in.) apart. Symmetric mounting flanges allowed the plug to be rotated such that the transducer rows were either "toward" (unfilled circles) or "away" (filled circles) from the fin leading edge (Fig. 4). Hence, measurements at several radial distances from the fin leading edge were possible.

The geometric data defining the transducer locations and orientation for all fin angles of attack are listed in Table 2. The radial distance r from the fin leading edge to the middle transducer in each row, normalized by the boundary-layer thickness, is tabulated along with the angle between the freestream direction and the normalized radius Ω. The middle transducers are no. 12 in row A and no. 10 in row B (see Fig. 4).

Measurements could be made with the transducer rows normal to the inviscid shock when the plug was rotated such that the rows were closest to the fin leading edge, $r/\delta \leq 3.28$. When the plug was installed with the rows farthest from the leading edge, $r/\delta \geq 4.59$, measurements could be made normal to the inviscid shock only for $\alpha \leq 22$ deg.

Discussion of Results

Surface Flow Visualization

Kerosene-lampblack surface flow visualization patterns were used to determine the angles of the separation and upstream influence lines. The method is described in Ref. 13. The angles were obtained by measuring the angle between the surface features outside of the inception region and a reference line in the freestream direction. The VCO was determined by finding the intersection point of a line drawn asymptotically to the separation line in the quasiconical far field and the inviscid shock trace extended ahead of the fin leading edge.

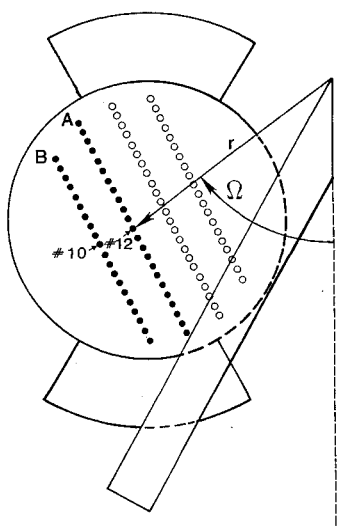

Fig. 4 Transducer plug.

Table 2 Orientation of transducer plug

Fin angle, α, deg	Inviscid shock angle, β_0, deg	Transducer row angle with respect to normal to freestream, deg	Normalized radial distance to transducer row, r/δ	Angle between freestream and normalized radius, Ω, deg
16	25.5	25.5	4.97	43.6
18	27.7	27.5	5.02	44.5
20	29.9	30	3.16	55.4
20	29.9	30	5.07	45.5
22	32.2	32	5.12	46.4
24	34.6	34.5	3.22	55.6
24	34.6	37	5.18	47.9
26	37.1	64	5.22	53.7
28	39.7	39.5	3.28	55.7
28	39.7	64	4.59	52.7
28	39.7	64	5.26	54.2

The surface feature angles compare favorably with those observed in previous studies. The upstream influence angle β_{ui} and primary separation line angle β_{s1} are plotted in Fig. 5, along with the empirical upstream influence angle correlation of Lu et al.[14] [Eq. (1)] and the upstream influence and separation angle correlations of Zheltovodov et al.[15] [Eqs. (2–4)]. Equations (3) and (4) are for separation with turbulent and laminar reverse flow, respectively:

$$\Delta\beta_{ui} = 2.2\Delta\beta_0 - 0.027\Delta\beta_0^2 \quad \text{where} \quad \Delta\beta = \beta - \mu_\infty \tag{1}$$

$$\beta_{ui} - \beta^*_{ui} = 1.53(\beta_0 - \beta^*_0) \quad \text{where} \quad \beta^*_{ui} = 1.22\beta^*_0 + 3.4 \tag{2}$$

$$\beta_{s1} - \beta^*_{s1} = 2.15(\beta_0 - \beta^*_0) - 0.0144(\beta_0 - \beta^*_0)^2$$

$$\text{where} \quad \beta^*_{s1} = \beta^*_0 \tag{3}$$

$$\beta_{s1} - \beta^*_{s1} = 1.94(\beta_0 - \beta^*_0) - 0.0154(\beta_0 - \beta^*_0)^2$$

$$\text{where} \quad \beta^*_{s1} = \beta^*_0 \tag{4}$$

In Eqs. (1–4), μ_∞ is the freestream Mach angle, β_0 is the inviscid shock wave angle, and the asterisk refers to surface feature angles at incipient separation.[15] For the current study the shock angle for incipient separation β^*_0 was determined to be 14 deg using the methods of Ref. 15. The correlations predict reasonably well the upstream influence and separation angles, with the exception of the strongest interactions, for which the correlations tend to underpredict the surface feature angles. This may be because the correlations were developed using data at Mach numbers between 2 and 4 and fin angles less than 30 deg, which would produce generally weaker interactions than those of the current study.

The experimentally determined VCO locations also followed trends observed by earlier investigators. As the strength of the interaction increased, the VCO approached the fin leading edge. This phenomenon had been observed in the previous work of Lu and Settles[16] at lower Mach numbers. Overall, the agreement between the surface features of the present and earlier investigations indicates that the experimental flowfield for the current study was effectively semi-infinite and free of irregularities.

Mean and Rms Pressure Distributions

Normalized mean wall pressure distributions in conical coordinates for α = 20, 24, and 28 deg are shown in Fig. 6. Note that the

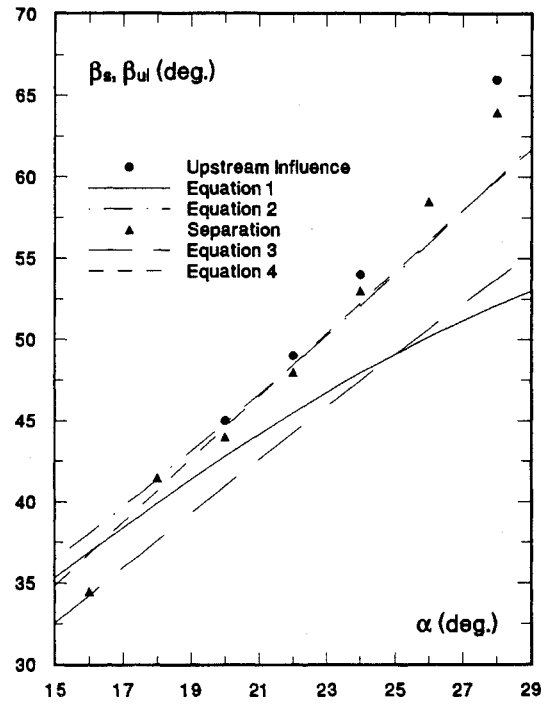

Fig. 5 Experimental surface feature angles and empirical correlations.

distributions for $\alpha = 24$ and 28 deg are offset vertically 2 and 4 units of $(\bar{P}_w/P_\infty)$ above the data for $\alpha = 20$ deg. The VCOs used to obtain β, the conical coordinates, are those determined from surface flow visualization. The locations of separation and the theoretical inviscid shock, S and β_0, are labeled, as is the theoretical inviscid pressure ratio across the shock. The latter is indicated by a horizontal bar on the pressure axis and takes into account the vertical offset of the data. The fin surface is indicated by a vertical bar to the left of each data set. Radial distances of the transducer rows, in terms of r/δ, are specified in the legend.

The quasiconical nature of the mean pressure field is quite evident despite the scatter in the data, which arises largely because transducers with relatively wide ranges (0–15 or 0–50 psia) were used to measure pressures that varied from about 0.6 to 5.5 psia (4.1×10^3 to 3.8×10^4 Pa). This was because the focus was on the fluctuating wall pressures, and high-frequency response transducers with stiff diaphragms are needed. Such transducers are not ideally suited to measuring the relatively low mean pressures encountered in these interactions.

The wall pressure standard deviation, normalized by the freestream static pressure and local mean wall pressure, is plotted in conical coordinates in Figs. 7 and 8, respectively. The VCOs are the same as those used in Fig. 6. It can be seen from Fig. 7 that load levels throughout the flowfield increase substantially with increasing angle of attack. From examination of both figures it can be stated with confidence that, within engineering accuracy, the rms pressure distributions, like the mean, are quasiconically symmetric. The skewness and flatness coefficient distributions are also quasiconically symmetric.[12] Note that the data for $\alpha = 28$ deg collapse well on the two inner rows, $r/\delta = 3.28$ and 4.59. On the outer row, $r/\delta = 5.26$, the rms levels are slightly higher than those on the two inner rows, possibly due to the influence of the sidewall interaction as discussed in Ref. 11.

The mean and rms pressure distributions are qualitatively the same as those measured by Gard and Settles[10] at low Mach numbers, except near the fin surface. Near the fin surface, Garg and Settles' distributions have maxima that are not visible at the higher Mach number of the current experiment. The maxima are defined by only one or two data points in the Mach 4 data but are well defined at Mach 3. A possible explanation has been presented by Alvi and Settles.[3] As the interaction strength increased, Alvi and Settles noticed that the flow structure became "compacted" into the junction of the fin and the test surface. This compression of the flowfield may cause features near the fin surface to become difficult to resolve in very strong interactions.

Intermittency

The fluctuating wall pressure signals near separation are intermittent, similar to those measured by Tran et al.[6] Samples of the wall pressure signals (≈1 record of 1024 points) between the upstream influence and separation line are shown in Fig. 9 for $\alpha = 16$,

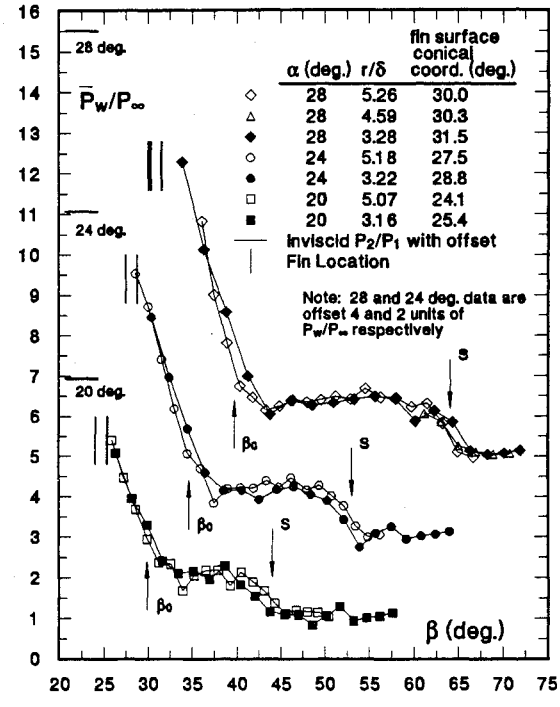

Fig. 6 Normalized mean surface pressure distributions in conical coordinates.

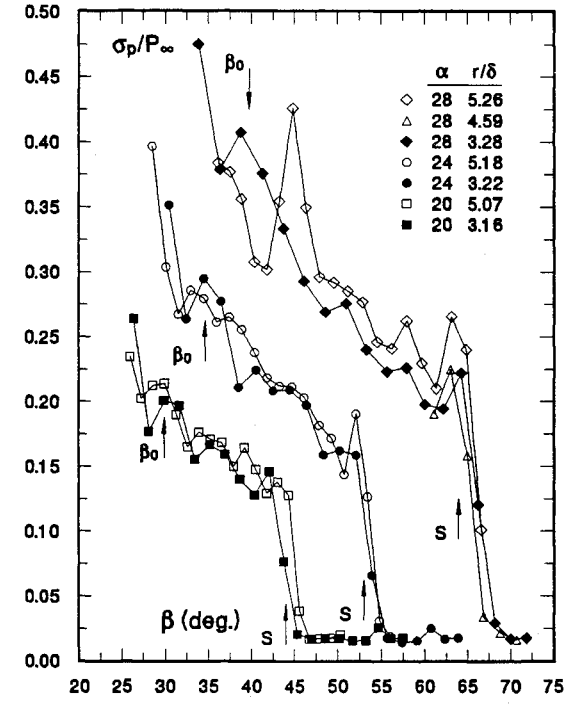

Fig. 7 Wall pressure standard deviation distribution in conical coordinates.

20, 24, and 28 deg. The calculated intermittencies, using the technique described in Ref. 17, are shown above each signal. The corresponding probability density distributions, calculated from 256 records, are shown in Fig. 10. In both figures the undisturbed boundary-layer data are shown for reference. Corroborating evidence of intermittency comes from the power spectra shown in Fig. 11, which show that the major contributor to the rms in the vicinity of separation is the large-amplitude fluctuations generated by the low-frequency motion of the separation shock wave. Calculations of separation shock zero-crossing frequency, again using the method of Ref. 17, give maximum values of 3–4 kHz that correlate well with the dominant frequencies in the spectrum. Because of the small size of the intermittent region, only three or fewer transducers could be placed within it; hence, detailed distributions of zero-crossing frequency could not be obtained. Thus, for fin angles between 16 and 28 deg, the upstream flowfield is characterized by a translating separation shock wave that generates an intermittent wall pressure signal.

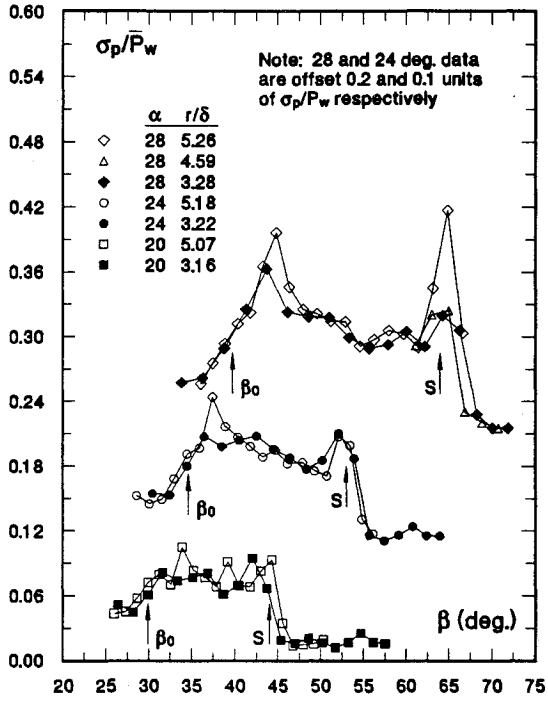

Fig. 8 Normalized standard deviation distribution in conical coordinates.

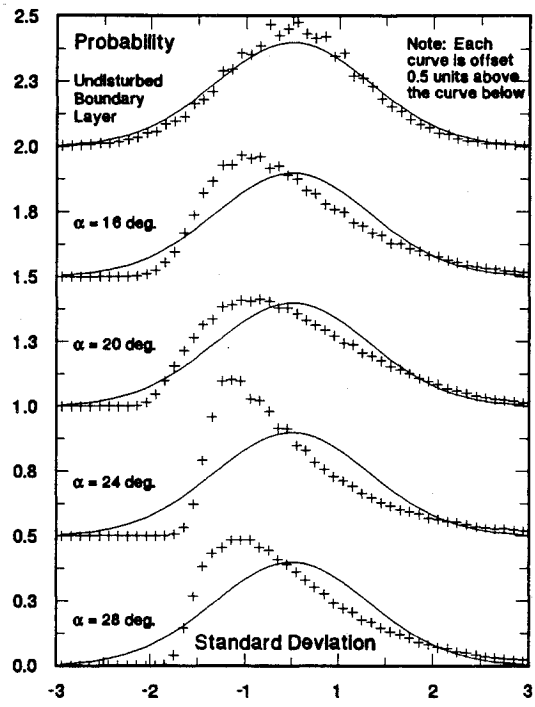

Fig. 10 Probability density distributions.

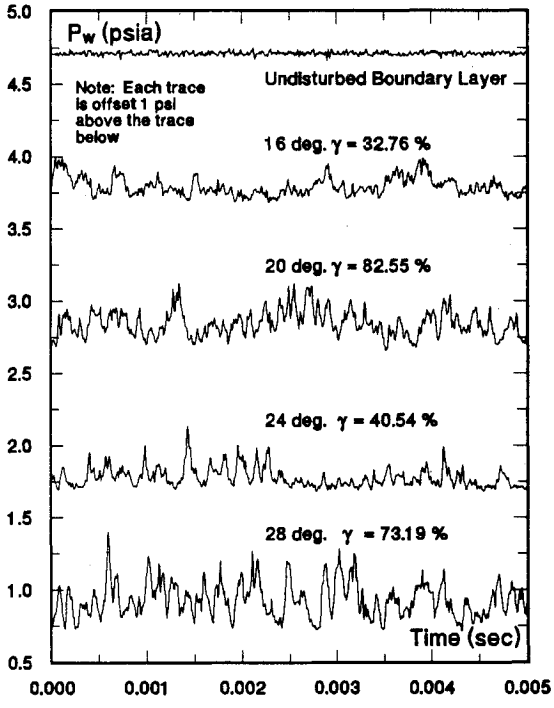

Fig. 9 Sample wall pressure signals near separation.

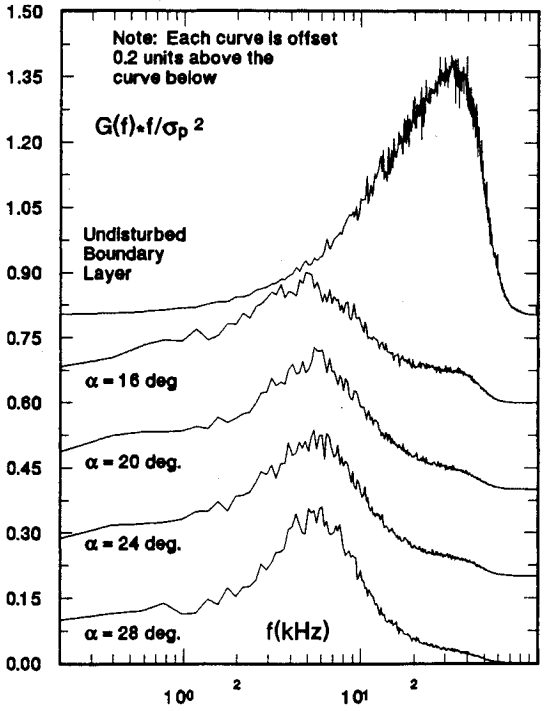

Fig. 11 Normalized power spectra.

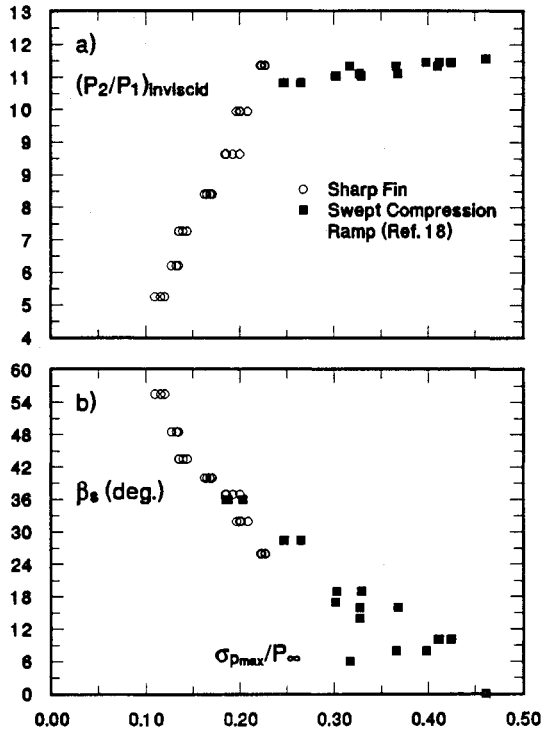

Fig. 12 Maximum standard deviation near separation as a function of a) inviscid pressure ratio and b) separation line sweep angle.

In light of the preceding findings, a pertinent question is why intermittent wall pressure signals were not detected in the earlier work of Gibson and Dolling[8,9] and the more recent work of Garg and Settles.[10] By comparing the flow conditions, flowfield scales and transducer arrangements of the aforementioned studies with those of Tran,[5] Tran, et al.,[6] Tan et al.,[7] and the present study, it appears that the measurements of Refs. 8–10 suffer from a combination of poor spatial resolution and comparatively weak separation shock strengths. For experiments with small intermittent regions in which a significant part of the shock motion may occur over a single transducer, the intermittent nature of the signal may be masked. Only when the shock wave moves completely upstream or downstream of the transducer, which occurs rarely, will the intermittent nature be evident and then only appear clearly if the separation shock is relatively strong. If the separation shock is weak such that the pressures upstream and downstream of it do not differ significantly, then the masking effect is exacerbated further. Thus, although poor spatial resolution or a weak shock alone will not necessarily mask the intermittency of the pressure signal, their combination may well do so. Although the sample signals in Fig. 9 are intermittent, it is still quite evident that the intermittency becomes more pronounced (and thus more readily detectable) with increasing angle of attack (i.e., increased separation shock strength and increased intermittent region length scale). The same observation was made by Tran et al.,[6] who noted that at Mach 3 intermittent characteristics were not apparent at $\alpha = 10$ deg, then appeared and increased in intensity as the fin angle was increased from 12 to 20 deg. Estimates of the VCO location were made using the data of Ref. 16, and the radial distance to the transducers from the VCO, R_{vco}, was determined for each study. The value of R_{vco} for Tran's[5] experiment was estimated to be 27.5 cm, over twice that for the other studies, which ranged from 11.4 to 12.8 cm. Thus, although the separation shock strengths of Tran[5] and Tran et al.[6] were weak, the intermittent characteristics of the wall pressure signal were evident because the intermittent region was large.

Since the work of Refs. 8 and 9 and the present study both originated within the same research group, the pressure signals of Refs. 8 and 9 could be re-examined. Recall that the data of Refs. 8 and 9 were obtained in the relatively thin boundary layer generated on a flat plate, whereas the measurements of the current study were made in the thicker boundary layer generated on the floor of the wind tunnel. Although the amplitude probability distributions of signals near separation in Refs. 8 and 9 are not significantly skewed, careful examination of the pressure signal itself indicates that it is indeed intermittent. As a result, the earlier conclusion of Refs. 8 and 9 that the signals in the initial compression region indicate a "shuddering" compression system are incorrect.

Influence of Sweep on Maximum Rms in Intermittent Region

It can be seen from Fig. 7 that the maximum rms generated by the separation shock σ_{pmax} increases with fin angle of attack. Because the sweepback of the interaction decreases and the overall strength of the interaction increases simultaneously as α is increased, it is not readily apparent which parameter causes the change in σ_{pmax}. The effects of sweepback and inviscid pressure rise can only be decoupled through comparisons of data for which the sweepback of the interaction was constant but the inviscid pressure rise was different and vice versa. The only data known to the authors that can be used to explore this issue are the swept compression ramp data of Erengil and Dolling.[18] Both the current fin and swept ramp studies were made in the same facility under practically identical freestream and boundary-layer conditions; hence, the only difference in the two is the geometry of the shock generator. In the work of Erengil and Dolling all ramps had a constant streamwise corner angle of 28 deg, whereas corner line sweepback angles ranged from 0 to 50 deg.

The normalized maximum rms pressure (σ_{pmax}/P_∞) near separation as a function of the overall inviscid pressure rise for both fin and ramp interactions is shown in Fig. 12a. Each configuration generates an approximately linear variation in σ_{pmax}/P_∞ with inviscid pressure rise but with different slopes. Although the data sets do not overlap, there is no physical reason to suppose that both data sets would undergo a radical change in slope and merge at a pressure ratio of about 11. The same data plotted as a function of separation line sweepback angle are shown in Fig. 12b. The relatively smooth decay of the data and their overlap strongly suggest that, for fixed incoming flow conditions, σ_{pmax} is primarily a function of the sweepback angle of (or Mach number normal to) the separation line. This result infers that σ_{pmax} is determined primarily by local flowfield structure near separation and not overall inviscid pressure rise. This inference has been confirmed by Gonsalez,[19] who has shown that σ_{pmax} in a wide variety of swept and unswept interactions is essentially equal to one-half of the separation shock wave strength. Depending on flowfield type, the latter may, or may not, be a function of overall inviscid pressure rise.

Conclusions

Fluctuating wall pressure measurements have been made in Mach 5 shock-wave/turbulent boundary-layer interactions generated by sharp, unswept fins at angles of attack of 16–28 deg. The experiment was conducted under approximately adiabatic wall temperature conditions. An attempt has been made to answer several questions regarding the radial evolution of the fluctuating pressure field, the unsteadiness of the compression system near separation, and how fluctuating pressure levels generated by the unsteady separation shock wave are affected by interaction sweepback. The results may be summarized as follows.

1) Using the virtual conical origin determined from surface flow visualization, it can be stated that within engineering accuracy both the mean and rms pressure distributions collapse quasiconically.

2) Visual inspection, time-series analysis, and conditional sampling of the fluctuating wall pressure signals between the upstream influence and separation lines indicate that the separation shock wave does generate an intermittent wall pressure signal, qualitatively similar to that seen in unswept interactions.

3) Although the maximum rms pressure near separation increases with increasing inviscid shock strength, as in swept compression ramp flows, comparison of data from the two types of flows strongly suggests that the appropriate correlating parameter is the interaction sweepback angle.

Acknowledgments

This work was funded in part by NASA Langley Research Center under Grant NAG2-1005 monitored by W. E. Zorumski. Support for the first author was also provided under the U.S. Air Force Palace Knight Program. These sources of support are gratefully acknowledged.

References

[1]Settles, G. S., and Dolling, D. S., "Swept Shock/Boundary-Layer Interactions—Tutorial and Update," AIAA Paper 90-0375, Jan. 1990.

[2]Alvi, F. S., and Settles, G. S., "Structure of Swept Shock Wave/Boundary-Layer Interaction Using Conical Shadowgraphy," AIAA Paper 90-1644, June 1990.

[3]Alvi, F. S., and Settles, G. S., "Physical Model of the Swept Shock/Boundary-Layer Interaction Flowfield," *AIAA Journal*, Vol. 30, No. 9, 1992, pp. 2252–2258.

[4]Knight, D., and Badekas, D., "On the Quasi-Conical Flowfield Structure of the Swept Shock Wave-Turbulent Boundary Layer Interaction," AIAA Paper 91-1759, June 1991.

[5]Tran, T. T., "An Experimental Investigation of Unsteadiness in Swept Shock Wave/Turbulent Boundary Layer Interactions," Ph.D. Dissertation, Mechanical and Aerospace Engineering Dept., Princeton Univ., Princeton, NJ, March 1987.

[6]Tran, T. T., Tan, D. K. M., and Bogdonoff, S. M., "Surface Pressure Fluctuations in a Three-Dimensional Shock Wave/Turbulent Boundary Layer Interaction at Various Shock Strengths," AIAA Paper 85-1562, July 1985.

[7]Tan, D. K. M., Tran, T. T., and Bogdonoff, S. M., "Wall Pressure Fluctuations in a Three-Dimensional Shock-Wave/Turbulent Boundary Interactions," *AIAA Journal*, Vol. 25, No. 1, 1987, pp. 14–21.

[8]Gibson, B. T., and Dolling, D. S., "Exploratory Study of Wall Pressure Fluctuations in a Mach 5, Sharp Fin-Induced Turbulent Interaction," *AIAA Journal*, Vol. 30, No. 9, 1992, pp. 2188–2195.

[9]Gibson, B., and Dolling, D. S., "Wall Pressure Fluctuations Near Separation in a Mach 5, Sharp Fin-Induced Turbulent Interaction," AIAA Paper 91-0646, Jan. 1991.

[10]Garg, S., and Settles, G. S., "Wall Pressure Fluctuations Beneath Swept Shock/Boundary Layer Interactions," AIAA Paper 93-0384, Jan. 1993.

[11]Schmisseur, J. D., and Dolling, D. S., "Unsteady Separation in a Sharp Fin-Induced Shock Wave/Turbulent Boundary Layer Interaction at Mach 5," AIAA Paper 92-0748, Jan. 1992.

[12]Schmisseur, J. D., "An Experimental Study of Fluctuating Wall Pressures in a Highly Swept, Sharp Fin-Induced, Mach 5 Shock Wave/Turbulent Boundary Layer Interaction," M.S. Thesis, Dept. of Aerospace Engineering and Engineering Mechanics, Univ. of Texas at Austin, Austin, TX, May 1992.

[13]Settles, G. S., and Teng, H. Y., "Flow Visualization of Separated 3-D Shock Wave/Turbulent Boundary Layer Interactions," *AIAA Journal*, Vol. 21, No. 3, 1983, pp. 390–397.

[14]Lu, F. K., Settles, G. S., and Horstman, C. C., "Mach Number Effects on Conical Surface Features of Swept Shock Boundary-Layer Interactions," *AIAA Journal*, Vol. 28, No. 1, 1990, pp. 91–97.

[15]Zheltovodov, A. A., Maksimov, A. I., and Shilein, E. K., "Development of Turbulent Separated Flows in the Vicinity of Swept Shock Waves," *The Interactions of Complex 3-D Flows*, edited by A. M. Kharitonov, USSR Academy of Sciences, Inst. of Theoretical and Applied Mechanics, Novosibirsk, Russia, 1987, pp. 67–91.

[16]Lu, F. K., and Settles, G. S., "Inception Length to a Fully-Developed Fin-Generated Shock Wave Boundary Layer Interaction," AIAA Paper 89-1850, June 1989.

[17]Marshall, T., and Dolling, D. S., "Comments on the Computation of Supersonic, Unswept, Turbulent Compression Ramp Interactions," *AIAA Journal*, Vol. 30, No. 8, 1992, pp. 2056–2065.

[18]Erengil, M. E., and Dolling, D. S., "Effects of Sweepback on Unsteady Separation in Mach 5 Compression Ramp Interactions," *AIAA Journal*, Vol. 31, No. 2, 1993, pp. 302–311.

[19]Gonsalez, J., "Correlation of Interaction Sweepback Effects on Unsteady Shock-Induced Turbulent Separation," M.S. Thesis, Dept. of Aerospace Engineering and Engineering Mechanics, Univ. of Texas at Austin, Austin, TX, Aug. 1993.